RSC Advances

PAPER

View Article Online
View Journal | View Issue

Cite this: *RSC Adv.*, 2022, **12**, 15150

Hydrothermal synthesis of Bi_2Se_3 nanosheets by using gallic acid as a reductant†

Di Huo, *[ab] Gongge Lin[a] and Mengfan Lv ‡[a]

In this work, a simple and reproducible hydrothermal synthesis was employed to synthesize two-dimensional Bi_2Se_3 nanosheets by using gallic acid as a reductant. Meanwhile, the effects of the amounts of gallic acid and sodium hydroxide and the surfactant Triton X-100 on phase composition and morphology of the obtained Bi_2Se_3 were also studied. The results reveal that gallic acid could effectively reduce Se^{4+} to Se^{2-} and gave rise to the formation of Bi_2Se_3. Additionally, keeping the reaction conditions of molar ratio of gallic acid to the precursor elements (Bi + Se) at 1 to 1 (or higher) and using strong alkaline solutions were the key factors to synthesize high purity crystalline Bi_2Se_3 nanosheets. Furthermore, flower-like Bi_2Se_3 composed of nanosheets with a dozen nanometer thickness could be easily fabricated by adding appropriate amounts of Triton X-100. This work provides a novel approach for synthesis of ultra-thin Bi_2Se_3 nanosheets in a controllable manner.

Received 20th February 2022
Accepted 11th May 2022

DOI: 10.1039/d2ra01129h

rsc.li/rsc-advances

1. Introduction

Bi_2Se_3, a VA-VIA direct semiconductor with a band gap E_g = 0.3 eV, has attracted much interest due to its great potential application in different fields such as optic-electronic sensitive devices,[1] room temperature thermoelectrics,[2] electrochemical hydrogen storage,[3] lithium battery electrodes[4] and photo-thermal therapy heating.[5] Additionally, Bi_2Se_3 is recognized as one of the typical topological materials which is insulating in the bulk but conducting on a surface with great potential usefulness in quantum computing and spintronic devices.[6,7] Bi_2Se_3 possesses the rhombohedral unit cell in which the equivalent atoms locate in a two-dimensional layer perpendicular to the *c*-axis. Five such layers arrange in the sequence of Se1–Bi–Se2–Bi–Se1. The Se atoms occupying two different sites form a tight bound unit that is termed quintuple layer (QL).[8] The chemical bonds between the QLs generally belong to van der Waals forces and the insides of these QLs are considered to be predominantly covalent. Thus, the characteristic of Bi_2Se_3 structure usually leads to sheets-like morphology because of anisotropic crystal growth. Many researches have shown that the physical and chemical properties of Bi_2Se_3 are well related to its crystal size and morphology. For example, the enhanced thermoelectric performances were achieved on nanostructured Bi_2Se_3 ceramics that were constituted of ultra-thin plates.[9,10] Therefore, it is important to synthesize Bi_2Se_3 with controlled crystal structure and morphology so as to realize the specific performances.

A number of techniques have been used in controlling synthesis of nanostructured Bi_2Se_3.[4,5,11–14] Therein the hydro/solvothermal synthesis was employed most popularly due to the advantages of simple, flexible, mild reactive condition and batch productivity. Meanwhile, crystal morphology of as synthesized samples can be controlled and modulated through changing reaction parameters including temperature, time, pH value, starting chemicals and surfactants. By now, Bi_2Se_3 with various morphologies such as nanoparticles, nanorods, nanobelts, and flowers-like have been fabricated by hydro/solvothermal route.[14–16] Even though successfully used in preparation of various nanostructured Bi_2Se_3, further improvement of hydro/solvothermal method needs to make is to exclude the utilization of many toxic and hazardous reducing agents such as $N_2H_4 \cdot H_2O$, $NaBH_4$, ethylenediamine and some organic chemicals that are detrimental to natural environments. There has been a few researches on trying the green synthesis to make nanostructured Bi_2Se_3,[17,18] but it is still necessary to develop novel synthetic route of nanostructured Bi_2Se_3 in a reliable and sustainable way.

Gallic acid (GA), or 3, 4, 5-trihydroxybenzoic acid with molecular formula $C_7H_6O_5$, is a naturally occurring polyphenolic compound which wildly distributes in various plants and natural herbs such as *Vitisvinifera*, *Syzagiumcordatum*, *Caesalpiniasappan*, and *Chinese gallnuts*, *Terminalia Chebulu Retz*.[19] It is also abundant in various fruits and beverages including walnut, strawberry, apple, grapes, green tea, and red

[a]*School of Materials Science and Engineering, Key Laboratory for Anisotropy and Texture of Materials (Ministry of Education), Northeastern University, Shenyang, 110819, Liaoning, PR China. E-mail: huod@atm.neu.edu.cn*

[b]*Advanced Ceramics Research Center, Department of Materials Science, Northeastern University, Shenyang, 110819, Liaoning, PR China*

† Electronic supplementary information (ESI) available. See https://doi.org/10.1039/d2ra01129h

‡ Present address: Advanced Institute of Information Technology PEKING University, Hangzhou 311215, Zhejiang, PR China.

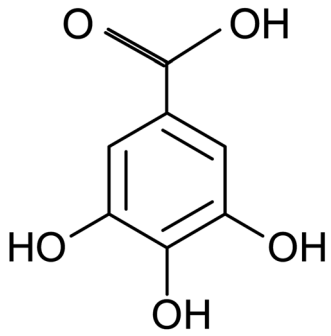

Fig. 1 Chemical structure of gallic acid.

wine.[20] GA in its free form or derivatives can be produced easily by extracting from natural plant sources or biosynthesis production at industrial level. As one of the natural active compounds, the biological and pharmacological properties of GA have been well recognized. Currently it is mainly used in fields of biomedicine and function food as antiviral, antibacterial and antioxidative agents.[19] Besides its important biochemical value, GA has also found wild applications in the packaging, cosmetic, and textile industries.[21] GA is a planar molecule that consists of an aromatic ring with three phenolic hydroxyl groups and a carboxylic acid group, as shown in Fig. 1. There are many chemical reaction pathways due to the existence of the active groups on it. It is generally believed that mild reducing effect of GA molecule comes from these phenolic hydroxyl groups in the process of chemical reaction in aqueous solutions.[20] Over the last few years, noble metallic particles including Au, Pt and Ag have been prepared using GA as reducing and capping agent,[22–24] and graphene oxide was also reduced to graphene by GA.[25] However, to the best of our knowledge there has been no report about preparing inorganic metal selenides nanosheets by using GA as reductant.

In this work, we report a novel green approach for hydrothermal synthesis of Bi_2Se_3 nanosheets by using GA as reductant and crystal growth modifier. Meanwhile, the effect of the amounts of GA, NaOH and Triton X-100 surfactant on composition and morphology of Bi_2Se_3 was also studied. Gram-scale, high crystallinity, ultrathin Bi_2Se_3 nanosheets were obtained in a controllable manner.

2. Experimental

All of the chemicals including Selinium dioxide (SeO_2, 99.99%), Bismuth nitrate pentahydrate ($Bi(NO_3)_3 \cdot 5H_2O$, 99.9%), Sodium hydroxide (NaOH, 99%), Gallic acid monohydrate and Triton X-100 purchased from Shanghai Aladdin Bio-Chem Technology Co., LTD were used without further treatment. The aqueous solutions were made using deionized water.

The hydrothermal synthesis procedure of Bi_2Se_3 nanosheets was as follows: firstly, NaOH (45 mmol, or 1.8 g) was dissolved in 70 ml deionized water under magnetic stirring at 70 °C for 3 min. Then, SeO_2 (6 mmol, or 0.6658 g) and $Bi(NO_3)_3 \cdot 5H_2O$ (4 mmol, or 1.9403 g) were added in sequence followed by further stirring for 20 min, and then, GA (10 mmol, or 1.8813 g) was added into the mixture solution accompanied by appropriate amount of Triton X-100 if necessary. After that, the mixed solution was transferred into a Teflon-lined autoclave of 100 ml capacity. The autoclave was sealed and maintained at 200 °C for 24 h and then allowed to cool to room temperature. The solid precipitate was separated by centrifugation, washed with deionized water for 3 times and absolute ethanol for 1 time, and finally about 1.2 g Bi_2Se_3 powder was obtained after drying at 60 °C for 8 h in vacuum. In order to control composition and to tailor morphology of the samples, GA was set in the range of 0.47–3.76 g; NaOH was of 0.6–2.4 g and Triton X-100 was of 0.005–5 g, respectively.

X-ray diffraction (XRD) pattern was carried out on a Japan Rigaku D/max X-ray diffractometer with graphite monochromatized Cu-Kα radiation ($\lambda = 1.54056$ Å) operating at tube voltage 40 KV and current of 20 mA. Field emission scanning electron microscopy (FE-SEM) image was taken on a Japan JEOL, JSM-7001F SEM to observe morphology of the samples. High resolution/Transmission electron microscopy (HRTEM/TEM) and selected area electronic diffraction (SAED) were performed with a Japan JEM-2100 F TEM at 100 kV accelerated voltage. X-ray energy dispersive spectroscopy (EDS) equipped on TEM was used to detect chemical elements of the samples. Fourier Transform Infrared (FTIR) spectra were performed with a RXI PerkinElmer spectrometer in the range of 500–4000 cm^{-1} at room temperature with the sample in a KBr disk. X-ray Photoelectronic Spectra (XPS) was collected on AXIS-SUPRA, Shimadzu-Kratos X-ray photoelectron spectrometer with Mono Al-Kα X-ray as the excitation source (1486.6 eV) to study chemicals and elemental valence of the products.

3. Results and discussion

3.1 Composition and morphology

First of all, the reduction effect of GA is illustrated on successful acquisition of the target compound after hydrothermal reaction. Fig. 2a shows XRD pattern of the product synthesized at 200 °C for 24 h. All diffraction peaks can be indexed in accordance with standard Bi_2Se_3 (JCPDS No 89-2008) with hexagonal structure of $a = b = 4.143$ Å, $c = 28.635$ Å. There are no any other phases left in the sample, which suggests pure Bi_2Se_3 is obtained. Fig. 2b shows the SEM image of Bi_2Se_3, almost all of the Bi_2Se_3 crystallizes in two-dimensional nanosheets-like morphology and some of them display clearly hexagonal plate shape with lateral length of 1–3 μm. It can be seen that a number of smaller sheet-like crystals grow out perpendicularly on surface of the basal hexagonal plates, which exhibit similar shapes as reported by Liu *et al.*[26] In most cases, the as synthesized Bi_2Se_3 grew into flower-like hierarchical nanostructures due to existence of dislocations generated in the process of Bi_2Se_3 growth.

HRTEM/TEM were used to further characterize the as synthesized Bi_2Se_3 nanosheets. As shown in Fig. 2c–e, the nanosheets keep smooth and approximate hexagonal flat shape, SAED analysis demonstrates its single crystalline nature, and the crystal lamellar distances within the single crystal zone on the HRTEM image are 3.04 Å and 2.06 Å, which is

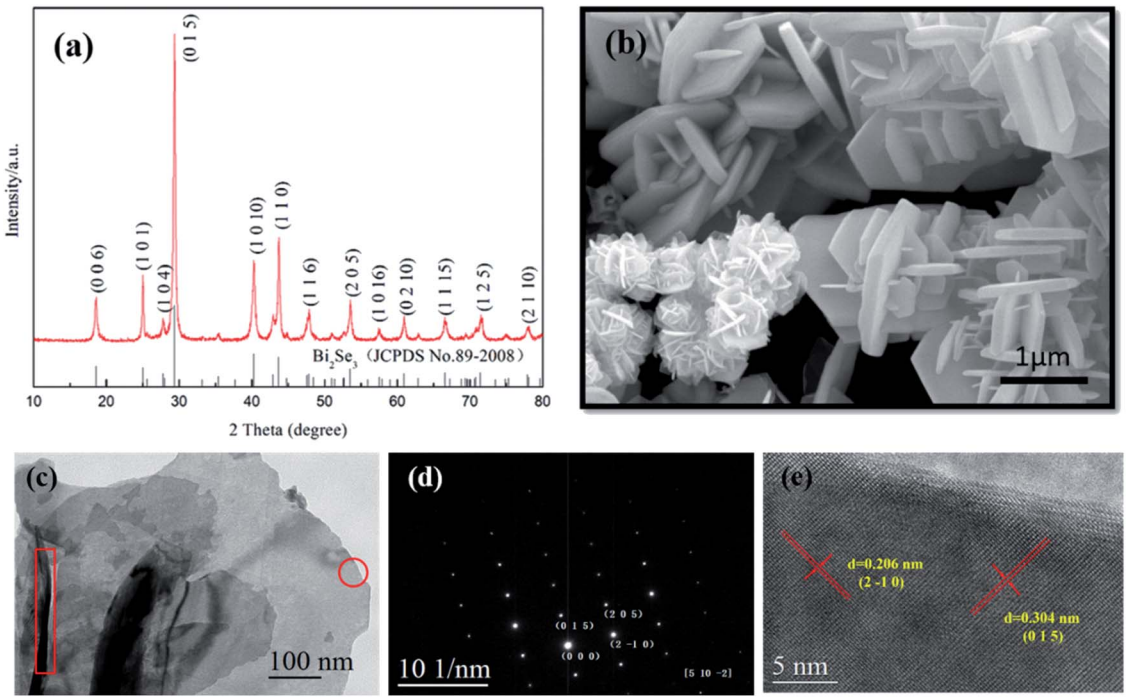

Fig. 2 (a) XRD pattern, (b) SEM, (c) TEM, (d) SAED and (e) HRTEM images of as synthesized Bi_2Se_3 nanosheets.

corresponding to (015) plane and (2$\bar{1}$0) plane of Bi_2Se_3, respectively. Although the precise thickness of the Bi_2Se_3 plates was not directly determined, it still can be seen that the estimated average thickness was about 30 nm, as indicated in red rectangle on TEM image.

Fig. 3a shows the FTIR spectrum of as synthesized Bi_2Se_3 nanosheets, it appears that there are various vibration absorption peaks arising from different chemical groups. The absorption at around 3349 cm^{-1} can be assigned to the stretching vibration of O–H banding which is brought about by phenolic hydroxyl of GA.[27] The other absorption peaks may be attributed to the residual organic groups or derivatives coming from the dissociated GA molecule under high pressure in hydrothermal reaction. For example, the peak appears at around 1355 cm^{-1} is attributed to C–O stretching vibration,[28,29] and the strongest absorption band at around 1620 cm^{-1} can be well assigned to the C=O stretching vibration of COOH group.[28–30] In addition, the absorption band at around 1851 cm^{-1} might be ascribed to the stretch vibration of C=O quinone carbonyl group conjugated to aromatic ring.[31] All of these FTIR absorption bands confirm the presence of organic residues from GA.

XPS calibrated with reference to C1s (bonding energy 284.8 eV) was carried out to evaluate the composition and chemical valence of as synthesized Bi_2Se_3. The wide scan spectrum confirms that element Bi, Se, C and O signals presenting in the product, among which C and O elements should originate from the organic acid residues (Fig. 3b). Except for these two elements, the obtained XPS scan spectrum is identical with that reported in other works.[13,32] The spectrum peaks of Bi 4*f* and Se 3*p* overlap at binding energy of about 160 eV, and the 4*f* have much higher intensities than the 3*p* transitions. In the fine spectrum of Bi element in Bi_2Se_3, the binding energy of Bi $4f_{7/2}$ at 157.9 eV and Bi $4f_{5/2}$ at 163.2 eV generate identical chemical shift of 1.3 eV compared to the binding energy at 156.6 eV and 161.9 eV of metallic Bi, with energy splitting of 5.3 eV (Fig. 3c). Similarly, the binding energy of Se $3d_{3/2}$ at 53.8 eV and Se $3d_{5/2}$ at 53.1 eV with energy splitting of 0.7 eV generate chemical shift of −1.5 eV and −1.4 eV, respectively, comparing to the binding energy at 55.3 eV and 54.5 eV of elemental Se (Fig. 3d). Additionally, Bi 4*d* levels with energy splitting of 23.5 eV can be observed in the spectrum. All of the features are accordance with the data that reported by other researchers,[32,33] indicating that pure Bi_2Se_3 compound is synthesized.

3.2 Effects of the processing parameters

Effect of GA amounts. It has been reported that many phenol derivatives are capable of reducing Fe^{3+} or Cu^{2+} to their lower oxidation state ions through redox reaction, in which di and trihydroxybenzens including GA are the most efficient reducers at pH 4.5.[34] Particularly, the reductive ability of GA molecules are known to increase with pH of the surrounding medium.[35] In this work, a parallel experiment in absence of GA was performed in order to verify GA's effect on the hydrothermal synthesis of Bi_2Se_3. The XRD pattern of the product is shown in Fig. 4a, all of the diffraction peaks can only be indexed to Bi_2O_3 (JCPDS No 65-2366), no any other phase can be observed in this product. Under the conditions of hydrothermal processing, $Bi(NO_3)_3 \cdot 5H_2O$ firstly reacts with NaOH to form $Bi(OH)_3$, which then further dehydrate to convert into Bi_2O_3 precipitates in strong alkaline solution.[36] On the other hand, SeO_2 would be dissolved in the alkaline solution resulting in formation of soluble

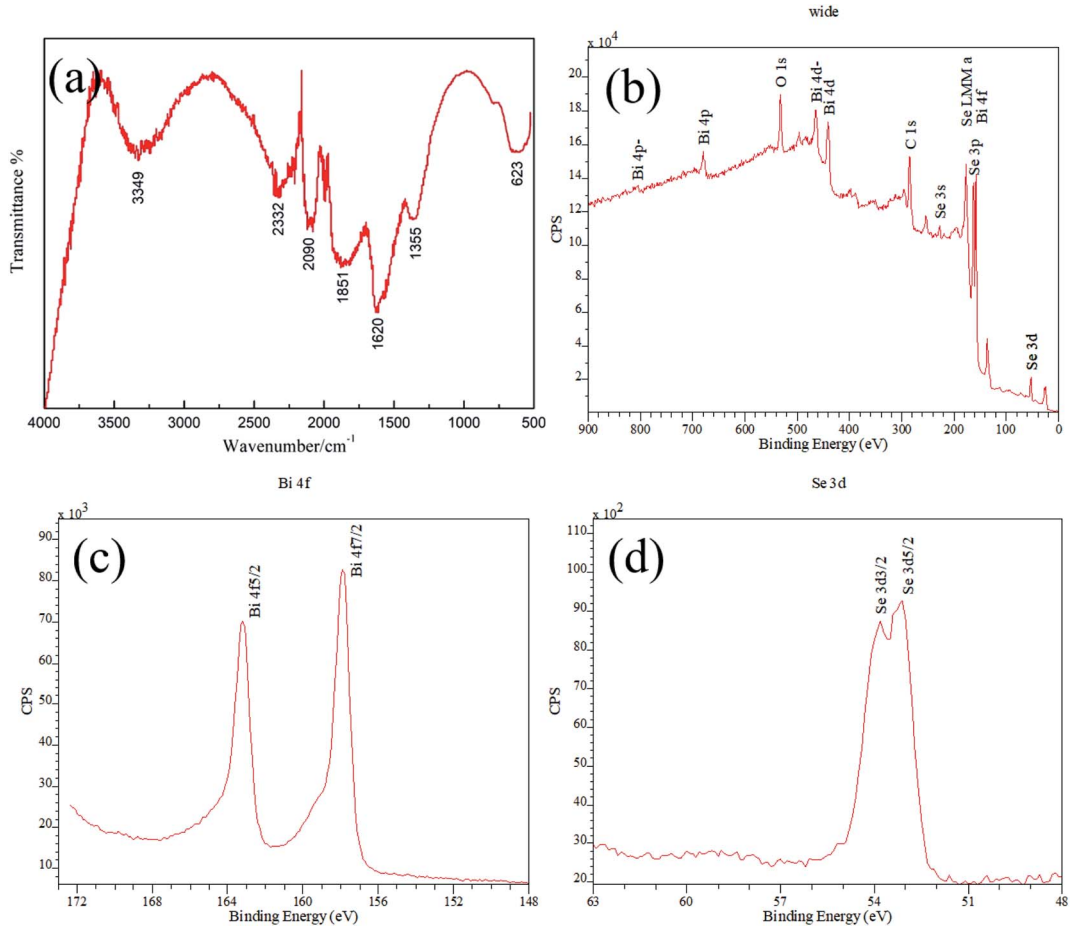

Fig. 3 (a) Infrared spectroscopy and XPS (b) wide scan spectrum, (c) Bi 4*f*, (d) Se 3*d* of as synthesized Bi_2Se_3.

selenious acid or other selenium species in the hydrothermal process. The result obtained in this work suggests that Se element did not react with Bi^{3+} to form Bi_2Se_3 but lost in the subsequent processing stage. Therefore, it is impossible to synthesize Bi_2Se_3 compound if GA is absent in the reaction solution. Different from nanosheets-like morphology of Bi_2Se_3, as shown in Fig. 4b, the formed Bi_2O_3 crystals have a rod-like shape with diameter of about 1 μm and length of 6 μm, which are similar to the one reported by other researchers.[36,37]

Based on the comparison experiment above, we can conclude that Bi_2Se_3 is generated by hydrothermal synthesis only when GA is present in solution. In order to understand the detailed effect of GA on phase composition and morphology, the samples with various GA contents were synthesized. The XRD patterns of these samples are shown in Fig. 5. Compared to

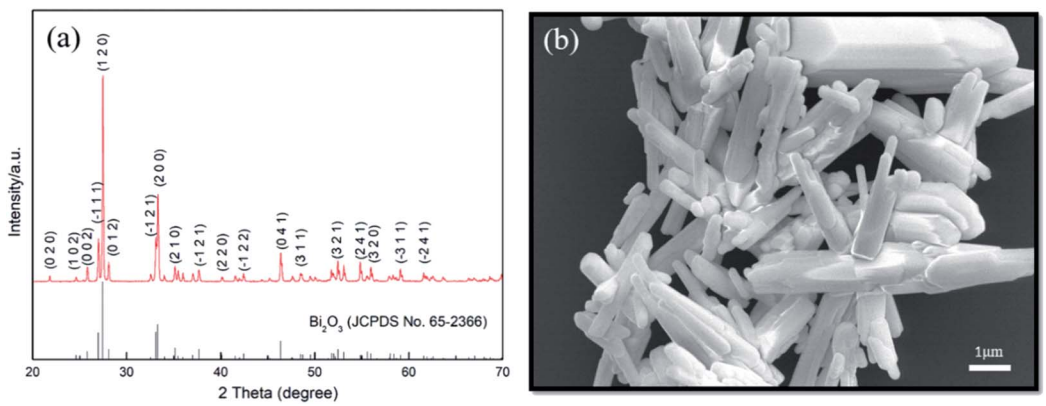

Fig. 4 (a) XRD pattern and (b) SEM image of Bi_2O_3.

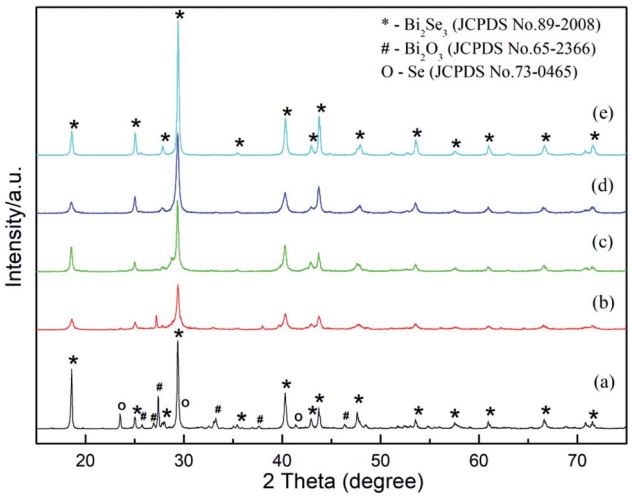

Fig. 5 XRD patterns of Bi_2Se_3 added various amount of GA. (a) 0.47 g, (b) 0.94 g, (c) 1.41 g, (d) 1.88 g, (e) 3.76 g.

the sample without adding GA, it can be seen the target compound Bi_2Se_3 appears promptly after adding GA. When 0.47 g GA was added (Fig. 5a), the phase composition of the product is consisted of dominated Bi_2Se_3, a small amount of Bi_2O_3 and trace of elemental Se (JCPDS No 73-0465). The diffraction peaks of Bi_2O_3 and Se become obviously less when GA content increases (Fig. 5b). When GA achieves at 1.41 g (Fig. 5c), the two intermediate phases disappear totally and only pure hexagonal Bi_2Se_3 exists. With further increasing of GA, as shown in Fig. 5d and e, the locations of diffraction peak keep unchanged except that their peaks become sharp as well as their HWFM become narrowed, which means highly crystallinity of Bi_2Se_3 is gotten. Therefore, adding sufficient amount of GA is necessary to provide enough reducing ability to finish the reaction. If setting the total precursor elements (Bi + Se) at a fixed value, the molar ratio of GA to the total elements had better to maintain at 1 to 1 (or higher) so that GA can reduce Se^{4+} to Se^{2-} completely for getting pure Bi_2Se_3.

The reductive effect of GA is generally believed coming from the phenolic hydroxyl groups of the molecular structure. GA is a strong natural antioxidant, and this property is related with the redox behavior.[19] The hydroxyl radicals bonded to benzene ring can be readily oxidized along with deprotonation and releasing of electrons, simultaneously. It is known that GA is oxidized to quinone *via* semiquinone form. The oxidation process of GA can precede by transferring one electron *via* the formation of semiquinone radical cation ($GA^{\bullet+}$), then the formed radical cation loses a proton to form the intermediate semiquinone radical ($GA^{\bullet}$), irreversibly. This reaction will be followed by a second irreversible electron transferring by forming quinine cation (GA^{+}), finally deprotonation of the quinine cation (GA^{+}) completes the overall two-electron process to give a quinine (GAO).[38] Therefore, here the released electrons from GA were transferred to Se^{4+} and the resulted Se^{2-} was used to form Bi_2Se_3 in the process of hydrothermal synthesis. The appearance of the strongest absorption peak of C=O radical in FTIR spectrograph may also support the presumption here.

It has been proposed that in strong alkaline medium the reduction process of Se^{4+} to Se^{2-} may proceed by either a two-step process of $Se^{4+} \rightarrow Se$ and $Se \rightarrow Se^{2-}$ or a one-step process of $Se^{4+} \rightarrow Se^{2-}$ by directly transferring six electrons.[39] It seems that the two-step mechanism worked in this experiment, because elemental Se was observed as an intermediate product in the process of hydrothermal reaction. Some Se^{4+} ions just finished the first part of the two-step reduction process when GA and NaOH contents were less than a certain value.

Based on the evolvement of phase components in XRD patterns (Fig. 5) and analysis above, the hydrothermal reaction pathway of Bi_2Se_3 formation might be outlined as follows. When GA is absent in solution, the reactions (1)–(3) carry out and only Bi_2O_3 is formed.

$$Bi(NO)_3 + NaOH \rightarrow Bi(OH)_3 + Na^+ + (NO)_3^- \quad (1)$$

$$SeO_2 + NaOH + H_2O \rightarrow Na_2SeO_3(\text{soluble}) + OH^- \quad (2)$$

$$2Bi(OH)_3 \xrightarrow{\text{hydrothermal in NaOH solution}} Bi_2O_3\downarrow + 3H_2O \quad (3)$$

On the contrary, when GA is present in solution, the reactions (4)–(8) occur and Bi_2Se_3 is obtained.

$$GA \rightarrow GA^{\bullet+} + e' \rightarrow GA^{\bullet} + e' + H^+ \quad (4)$$

$$GA^{\bullet} \rightarrow GAO + e' + H^+ \quad (5)$$

$$Se^{4+} + 4e' \rightarrow Se \quad (6)$$

$$Se + 2e' \rightarrow Se^{2-} \quad (7)$$

$$3Se^{2-} + 2Bi(OH)_3 \xrightarrow{\text{hydrithermal in NaOH solution}} Bi_2Se_3\downarrow + 6(OH)^- \quad (8)$$

It is necessary to note that theoretically electrochemical reduction potential of Se ($E^{o}_{Se/se^{2-}_{Se/se}}$) is −0.924 V,[39] and cyclic voltammogram (CV) electrochemical measurement for GA has confirmed reductive potentials of −1.20 V, −1.44 V, −1.65 V and −1.90 V for each hydroxyl group and carboxylic acid group in a strong alkaline solution.[35] So increasing GA concentration are obviously favorable for completing the whole two-step reduction of Se^{4+} to Se^{2-} and forming Bi_2Se_3 in terms of electrochemical reduction potentials, especially at high concentration of NaOH.

Besides the capability of reducing Se^{4+} to Se^{2-} state, GA can also alter morphology of as synthesized Bi_2Se_3. With addition of 0.47 g GA, mixed morphologies composing predominated platelets are observed (Fig. 6a). When the GA contents continuously increase to 1.41 g and then to 1.88 g, nanosheets-like morphology of Bi_2Se_3 crystals become more prominence, as illustrated by their larger plate areas and thinner thickness. Additionally, their flower-like characteristics become obviously (Fig. 6b and c). However, when further increasing GA contents up to 2.35 g and 2.82 g (Fig. 6d and e), nanosheets-

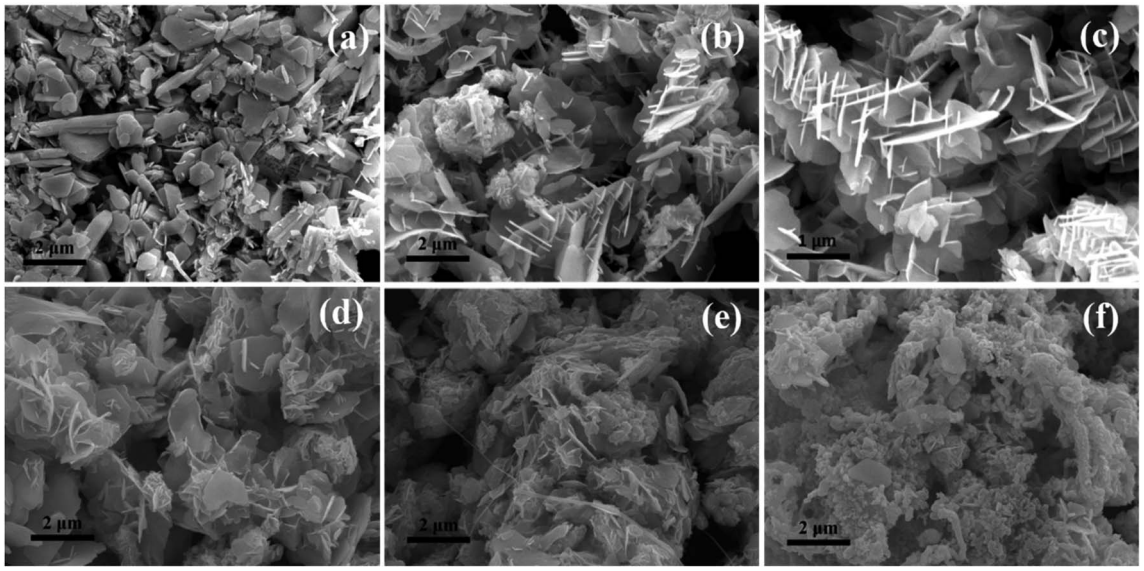

Fig. 6 SEM images of samples added different amounts of GA. (a) 0.47 g, (b) 1.41 g, (c) 1.88 g, (d) 2.35 g, (e) 2.82 g, (f) 3.76 g.

like morphologies gradually disappear. As adding 3.76 g GA, irregular agglomerated Bi_2Se_3 nanoparticles with few layered particles emerge in the sample (Fig. 6f). High concentration of GA will accelerate the reductive rate of Se^{4+} to Se^{2-} and boost the reaction kinetics of Bi_2Se_3 formation. Thus, a large number of Bi_2Se_3 crystals nucleate in short time, these nucleus aggregate together quickly rather than grow into nanosheets in an anisotropic manner. In addition, when the amount of GA is excessive in solution, the freshly formed surface of inorganic Bi_2Se_3 particles may be covered by GA molecule or its derivatives, which may also lead to the inhibition of directional crystal growth. Overall, the suitable amount of GA for controllable synthesis of Bi_2Se_3 nanosheets are in range of 1.41 g ~2.35 g.

Effect of NaOH. Oxidative capability of polyphenol acids is directly related to pH value of its surrounding medium.[19] It has been confirmed that GA is quite susceptible to oxidation at pH >7, for example, hydroxyl radicals can directly induce the oxidation of GA at pH of 12 and 13.6.[40] Hence, the quantity of NaOH added in the solution immensely affects hydrothermal synthesis process of Bi_2Se_3.

Fig. S1† shows the XRD pattern of the samples added with different amounts of NaOH. When adding 0.6 g NaOH, the product is consisted of dominated Bi_2Se_3 with minor elemental Se residues, but none Bi_2O_3 exists (Fig. S1a†). Low concentration of NaOH does not only slow the degree of oxidation of GA, which may lead to poor reductive efficiency of Se → Se^{2-}, but also make the precipitations of Bi_2O_3 unfavorable. When NaOH increases up to 1.2 g or above, hexagonal Bi_2Se_3 phase with high crystallinity is obtained, as shown in Fig. S1(b–d).†

Increasing the amount of NaOH or pH value of hydrothermal solution is beneficial for the formation of Bi_2Se_3 due to enhanced reducing ability of GA. Meanwhile, it shows that crystal morphologies of Bi_2Se_3 changes accordingly with different alkaline degree in aqueous solution (Fig. S2†). Apparently, the flat surface area of Bi_2Se_3 nanosheets increases with increasing amounts of NaOH. In Fig. S2a,† the nanoparticles dispersing on surfaces of Bi_2Se_3 nanosheets added with 0.6 g NaOH might be attributed to elemental Se, as indicated in the XRD pattern in Fig. 6. The rates of nucleation and crystal growth will be thermodynamic accelerated under the strong alkaline condition during synthesizing nanostructured chalcogenides.[41] Similarly, the formation of Bi_2Se_3 would be facilitated as NaOH contents increase in solution, and then leading to the enlarged flat areas and decreased thickness of layered Bi_2Se_3 nanosheets. Their shapes become nearly hexagonal plate-like in the end, as shown in Fig. S2(b–d).†

Effect of surfactant triton X-100. A common and effective way to modulate crystal growth in aqueous solution is to use surfactant agents. Nonionic type surfactant Triton X-100 containing both hydrophobic and hydrophilic group is of high stability in water without ionization, it also shows good compatibility with GA molecule.[42] Triton X-100 has used successfully to control anisotropic crystal growth as morphology modulator and act as dispersing agent to prevent layer stacking of MoS_2.[43] Here ultrathin Bi_2Se_3 nanosheets with a dozen of nanometer thickness was synthesized when adding appropriate amounts of Triton X-100 in hydrothermal reaction system. First, the pure hexagonal Bi_2Se_3 phase kept unchanged as implied in the XRD patterns after adding various amounts of Triton X-100 (Fig. S3†). Furthermore, it deserves noted that the diffraction peak intensity ratio ($I_{(006)}/I_{(015)}$) of (006) plane to (015) plane increased with increasing of Triton X-100, *i.e.*, $I_{(006)}/I_{(015)}$ increased from 0.18 to 0.28 as the surfactant increased from 0.05 g to 0.625 g, which might suggest the crystallinity of (006) plane was enhanced.

Fig. 7 shows SEM images of Bi_2Se_3 added with various amounts of Triton X-100. When 0.05 g Triton X-100 was added, the thickness of Bi_2Se_3 nanosheets started to decrease

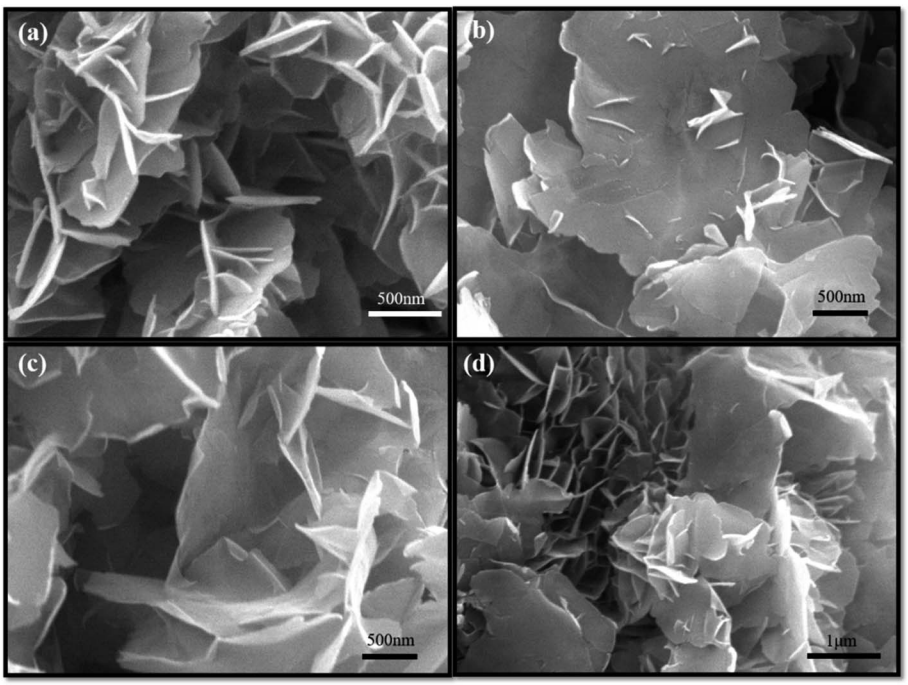

Fig. 7 SEM images of samples with different amount of Triton X-100. (a) 0.05 g; (b) 0.2 g; (c) 0.625 g; (d) 5 g.

obviously (Fig. 7a). With continuously adding Triton x-100 to 0.2 g and further to 0.625 g, the plate area increases and the thickness decreases, accordingly. The size of a single nanosheet is about 3 μm in wide and a dozen of nanometer in thickness (Fig. 7b and c). As the surfactant increased up to 5 g, the lateral wide and thickness of the ultrathin nanosheets remain unchanged essentially (Fig. 7d). It is reasonable to postulate that hydrophobic side of the amphiprotic Triton X-100 absorbs directionally on nanosheets surfaces, thus forming ultrathin Bi_2Se_3 nanosheets with mainly lateral crystal growth. On the other hand, the hydrophilic side of Triton X-100 played a role on dispersion that led to less aggregation of Bi_2Se_3 nanosheets. From the TEM image, one can find much smoother and less curved plate-like characteristic of these ultrathin Bi_2Se_3 nanosheets. The SAED proves its single crystalline nature and EDS analysis features standard Bi/Se molar ratio of 2/3 (Fig. S4†).

4. Conclusions

In this work, we develop a simple and reproducible hydrothermal synthesis method for preparing Bi_2Se_3 nanosheets, in which GA is used as reductant to reduce Se^{4+} to Se^{2-} and then the Se^{2-} ion further reacts with Bi^{3+} to form Bi_2Se_3. Along with the reducing effect, GA molecule can change the morphology of as synthesized Bi_2Se_3. It was also found that keeping sufficient amounts of GA and NaOH in hydrothermal reaction system are the key factors to the synthesis of pure crystalline Bi_2Se_3 nanosheets, and thinner Bi_2Se_3 nanosheets with a dozen of nanometer thickness can be easily synthesized when adding appropriate amount of non-ionic surfactant Triton X-100.

5. Author contributions

Di Huo: Conceptualization, Methodology, Investigation, Writing-review & editing, Funding acquisition, Supervision. Gongge Lin: Performing experiments, Validation. Mengfan Lv: Performing experiments, Data collection.

Conflicts of interest

There are no conflict of interests to declare.

Acknowledgements

The authors acknowledge Dr Yujie Liu for assistance on TEM operation and Dr Junqing Xia for collecting XPS data. This work was funded in part by National Nature Science Foundation of China (No 51872033).

References

1 A. K. Rath, M. Bernechea, L. Martinez and G. Konstantatos, *Adv. Mater.*, 2011, **23**, 3712–3717.
2 W. Liu, K. Lukas, K. McEnaney, S. Lee, Q. Zhang, C. P. Opeil, G. Chen and Z. F. Ren, *Energy Environ. Sci.*, 2013, **6**, 552–560.
3 Z. Sun, F. Liu, X. Chen and L. Chen, *Chem. Commun.*, 2010, **46**, 3101–3103.
4 H. M. Xu, G. Chen, R. C. Jin, J. Pei, Y. Wang and D. H. Chen, *CrystEngComm*, 2013, **15**, 1618–1625.
5 H. Zhou, L. Che, Z. M. Guo, M. H. Wu, W. Q. Li, W. P. Xu and L. F. Liu, *ACS Sustainable Chem. Eng.*, 2018, **6**, 4863–4870.

6 M. Salvato, M. Scagliotti, M. de Crescenzi, P. Castrucci, F. de Matteis, M. Crivellari, S. PelliCresi, D. Catone, T. Bauch and F. Lombardi, *Nanoscale*, 2020, **12**, 12405.
7 L. A. Wray, S. Y. Xu, Y. Q. Xia, Y. S. Hor, D. Qian, A. V. Fedorov, H. Lin, A. Bansil, R. J. Cava and M. Z. Hasan, *Nat. Phys.*, 2010, **6**, 855–859.
8 Z. G. Chen, G. Han, L. Yang, L. Cheng and J. Zou, *Prog. Nat. Sci.: Mater. Int.*, 2012, **22**, 535–549.
9 C. Bauer, I. Veremchuk, C. Kunze, A. Benad, V. M. Dzhagan, D. Haubold, D. Pohl, G. Schierning, K. Nielsch, V. Lesnyak and A. Eychmüller, *Small Sci.*, 2020, **1**, 2000021.
10 M. Hong, Z. G. Chen, L. Yang, G. Han and J. Zou, *Adv. Electron. Mater.*, 2015, **1**, 1500025.
11 R. Harpeness and A. Gedanken, *New J. Chem.*, 2003, **27**, 1191–1193.
12 H. M. Cui, H. Liu, X. Li, J. Y. Wang, F. Han, X. D. Zhang and R. I. Boughton, *J. Solid State Chem.*, 2004, **177**, 4001–4006.
13 J. R. Ota, P. Roy, S. K. Srivastava, R. Popovitz-Biro and T. Reshef, *Nanotechnology*, 2006, **17**, 1700–1705.
14 B. Belec, K. Ferfolja, T. Goršak, N. Kostevšek, S. Gardonio, M. Fanetti and M. Valant, *Sci. Rep.*, 2019, **9**, 19057.
15 H. Fan, S. X. Zhang, P. Ju, H. C. Su and S. Y. Ai, *Electrochim. Acta*, 2012, **64**, 171–176.
16 Y. Xie, H. Su, B. Li and Y. T. Qian, *Mater. Res. Bull.*, 2000, **35**, 459–464.
17 M. Kuroda, S. Suda, M. Sato, H. Ayano, Y. Ohishi, H. Nishikawa, S. Soda and M. Ike, *Appl. Microbiol. Biotechnol.*, 2019, **103**, 8853–8861.
18 H. M. Xu, G. Chen, R. C. Jin, D. H. Chen, Y. Wang and J. Pei, *RSC Adv.*, 2014, **4**, 8922–8929.
19 B. Badhani, N. Sharma and R. Kakkar, *RSC Adv.*, 2015, **5**, 27540.
20 S. Dhiman and M. Mukherjee, Gallic acid (GA): A multifaceted biomolecule transmuting the biotechnologu era, in *Recent Developments in microbial Technologies, Environmental and Microbial Biotechnology*, ed. R. Prasad, Spinger Natural Singapore Pte Ltd, 2021, pp. 163–202.
21 B. R. Albuquerque, S. A. Heleno, M. B. Oliveira, L. Barros and I. C. R. Ferraira, *Food Funct.*, 2021, **12**, 14.
22 K. Yoosaf, B. I. Ipe, C. H. Suresh and K. G. Thomas, *J. Phys. Chem. C*, 2007, **111**, 12839–12847.
23 G. A. Martinez-Castanon, N. Nino-Martinez, F. Martinez-Gutierrez, J. R. Martinez-Mendoza and F. Ruiz, *J. Nanopart. Res.*, 2008, **10**, 1343–1348.
24 K. M. Kumar, B. K. Mandal and S. K. Tammina, *RSC Adv.*, 2013, **3**, 4033.
25 J. Li, G. Y. Xiao, C. B. Chen, R. Li and D. Y. Yan, *J. Mater. Chem. A*, 2013, **1**, 1481.
26 X. L. Liu, J. W. Xu, Z. C. Fang, L. Lin, Y. Qian, Y. C. Wang, C. M. Ye, C. Ma and I. Zeng, *Nano Res.*, 2015, **8**, 3612–3620.
27 F. Billes, I. Mohammed-Ziegler and P. Bombicz, *Vib. Spectrosc.*, 2007, **43**, 193–202.
28 G. Cirillo, S. Hampel, R. Klingeler, F. Puoci, F. Iemma, M. Curcio, O. I. Parisi, U. G. Spizzirri, N. Picci, A. Leonhardt, M. Ritschel and B. Büchner, *J. Pharm. Pharmacol.*, 2011, **63**, 179–188.
29 K. M. Kumar, B. K. Mandal and S. K. Tammina, *RSC Adv.*, 2013, **3**, 4033–4039.
30 A. H. Nadim, M. A. Al-Ghobashy, M. Nebsen and M. A. Shehata, *RSC Adv.*, 2015, **5**, 104981–104990.
31 P. R. Griffiths and J. A. de Haseth, *Fourier transform infrared spectroscopy*, John wiley& Sons, Hoboken, NJ, 1986.
32 M. R. Thuler, R. L. Benbow and Z. Hurych, *Chem. Phys.*, 1982, **71**, 265–270.
33 V. B. Nascomento, V. E. de Carvslho, R. Paniago, E. A. Soares, L. O. Ladeira and H. D. Pfannes, *J. Electron Spectrosc. Relat. Phenom.*, 1999, **104**, 99–107.
34 A. Aguiar and A. Ferraz, *Chemosphere*, 2007, **66**, 947–954.
35 M. K. Carter, *J. Mol. Struct.*, 2007, **831**, 26–36.
36 C. Wu, L. Shen, Q. L. Huang and Y. C. Zhang, *Mater. Lett.*, 2011, **65**, 1134–1136.
37 M. Muruganandham, R. Amutha, G. J. Lee, S. H. Hsieh, J. Wu and M. Sillanpää, *J. Phys. Chem. C*, 2012, **116**, 12906–12915.
38 R. Abdel-Hamid and E. F. Newair, *J. Electroanal. Chem.*, 2011, **657**, 107–112.
39 M. Bouroushian, *Electrochemistry of Metal Chalcogenides*, Springer-Verlag Berlin, Heidelberg, 2010.
40 P. Dwibedy, G. R. Dey, D. B. Naik, K. Kishore and P. N. Moorthy, *Phys. Chem. Chem. Phys.*, 1999, **1**, 1915–1918.
41 Y. H. Wang, J. Zhang, Y. L. Yang, F. Huang, J. S. Zheng, D. G. Chen, F. B. Yang, Z. Lin and C. Wang, *J. Phys. Chem. B*, 2007, **111**, 5290–5294.
42 A. M. Campos, E. Ponce and E. A. Lissi, *J. Phys. Org. Chem.*, 2009, **22**, 1208–1211.
43 G. Kedawat, P. Kumar, K. Nagpal, S. J. Paul, V. N. Singh, S. S. Kumar and B. K. Gupta, *ChemistrySelect*, 2019, **4**, 6219–6226.